Journal of Intelligent & Robotic Systems (2026) 112:20
https://doi.org/10.1007/s10846-026-02351-7

RESEARCH

SMapper: A Multi-Modal Data Acquisition Platform for SLAM Benchmarking

Pedro Miguel Bastos Soares[1] · Ali Tourani[1,2] · Miguel Fernandez-Cortizas[1] · Asier Bikandi-Noya[1] · Holger Voos[1,3] · Jose Luis Sanchez-Lopez[1]

Received: 10 October 2025 / Accepted: 7 January 2026

Abstract

Advancing research in fields such as Simultaneous Localization and Mapping (SLAM) and autonomous navigation critically depends on the availability of reliable and reproducible multimodal datasets. While several influential datasets have driven progress in these domains, they often suffer from limitations in sensing modalities, environmental diversity, and the reproducibility of the underlying hardware setups. To address these challenges, this paper introduces *SMapper*, a novel open-hardware, multi-sensor platform designed explicitly for, though not limited to, SLAM research. The device integrates synchronized LiDAR, multi-camera, and inertial sensing, supported by a robust calibration and synchronization pipeline that ensures precise spatio-temporal alignment across modalities. Its open and replicable design allows researchers to extend its capabilities and reproduce experiments across both handheld and robot-mounted scenarios. To demonstrate its practicality, we additionally release *SMapper-light*, a publicly available SLAM dataset containing representative indoor and outdoor sequences. The dataset includes tightly synchronized multimodal data and ground truth trajectories derived from offline LiDAR-based SLAM with sub-centimeter accuracy, alongside dense 3D reconstructions. Furthermore, the paper contains benchmarking results on state-of-the-art LiDAR and visual SLAM frameworks using the *SMapper-light* dataset. By combining open-hardware design, reproducible data collection, and comprehensive benchmarking, *SMapper* establishes a robust foundation for advancing SLAM algorithm development, evaluation, and reproducibility. The project's documentation, including source code, CAD models, and dataset links, is publicly available at https://snt-arg.github.io/smapper_docs/.

Keywords Dataset · SLAM · Sensor fusion · Robotics

1 Introduction

Collecting reliable high-quality data is a critical task in robotics research, driving progress in autonomous navigation, Simultaneous Localization and Mapping (SLAM), and enhancing robots' perceptual and situational awareness [1]. Such data instances not only provide the foundation for developing novel algorithms against precise ground truth, but also serve as benchmarks for comparing diverse approaches, ensuring that robotic systems can operate robustly across diverse environments [2, 3]. In particular, progress in SLAM critically depends on access to multimodal data collected across dissimilar scenarios, where evaluation under varying motion dynamics, lighting conditions, and structural layouts is essential for achieving robustness, accuracy, and generalization [4, 5].

During the past decade, several influential and practical datasets, such as KITTI [6], EuRoC [7], and TUM RGB-D [8], have significantly shaped the field of SLAM and served as evaluation benchmarks for many developed systems. However, they often face limitations in sensing modalities, environmental diversity, and the availability of reproducible hardware setups for further data collection. As a result, the fixed nature of existing data instances constrains researchers and industries, making it challenging to replicate sensor configurations or extend them to new scenarios.

To address such challenges, multimodal sensing has emerged as a reliable solution to advance SLAM data collection and processing [9]. While unimodal sensors such as visual sensors (*e.g.,* monocular, stereo, RGB-D, or event cameras), Light Detection And Ranging (LiDAR), and Inertial Measurement Units (IMUs) provide the fundamental measurements for SLAM, integrating them into multimodal configurations adds complementary data streams that enable

Pedro Miguel Bastos Soares and Ali Tourani contributed equally.

Extended author information available on the last page of the article

Published online: 28 January 2026

more robust, accurate, and reliable system development [10]. Additionally, these sensing modalities are often complemented by external systems, such as Motion Capture System (MCS) or GPS, which provide accurate ground truth reference trajectories for SLAM evaluation and benchmarking [11]. However, most existing efforts do not release both the *collected datasets* and the *underlying hardware design*, leaving a gap in reproducibility and extensibility for the SLAM community.

This paper presents *SMapper*, a novel, multi-sensor, open-hardware platform specifically designed for data collection in SLAM, covering visual, LiDAR, and multi-sensor SLAM variants. The platform integrates synchronized visual, LiDAR, and inertial sensing, and can be replicated by researchers owing to its open hardware specification and detailed technical documentation. Furthermore, we release a publicly available Visual SLAM (VSLAM) dataset to demonstrate the practicality of the platform for benchmarking and evaluation. The dataset includes trajectories derived from visual, inertial, and LiDAR sensing, where the LiDAR data are processed using a high-accuracy LiDAR SLAM system to generate trajectory estimates that serve as the ground truth reference for evaluating visual–inertial SLAM. An overview of the proposed *SMapper* device is presented in Fig. 1, depicting both the fully assembled physical prototype and the inner sensor and component configuration designed for comprehensive data acquisition.

With these, the paper offers the following contributions:

- A compact, open-hardware, and fully synchronized multimodal SLAM data collection platform, integrating LiDAR, IMU, and visual sensors, supporting both handheld and robot-mounted configurations,
- A publicly available multimodal dataset for VSLAM, accompanied by benchmarking results to depict the platform's performance across diverse scenarios; and
- An open-source software suite for sensor calibration, data acquisition, and real-time monitoring, facilitating reproducible and efficient data collection.

The remainder of the paper is structured as follows: Section 2 reviews related works and various dataset collection setups for SLAM. In Section 3, the design and technical specifications of the proposed device are detailed. Section 4.2 outlines the data collection methodology and setup, with benchmarking results and evaluations presented in Section 4. The paper concludes and discusses potential directions for future work in Section 5.

2 Related Works

Many efforts have explored diverse sensing modalities to collect reliable experimental and ground truth data for the

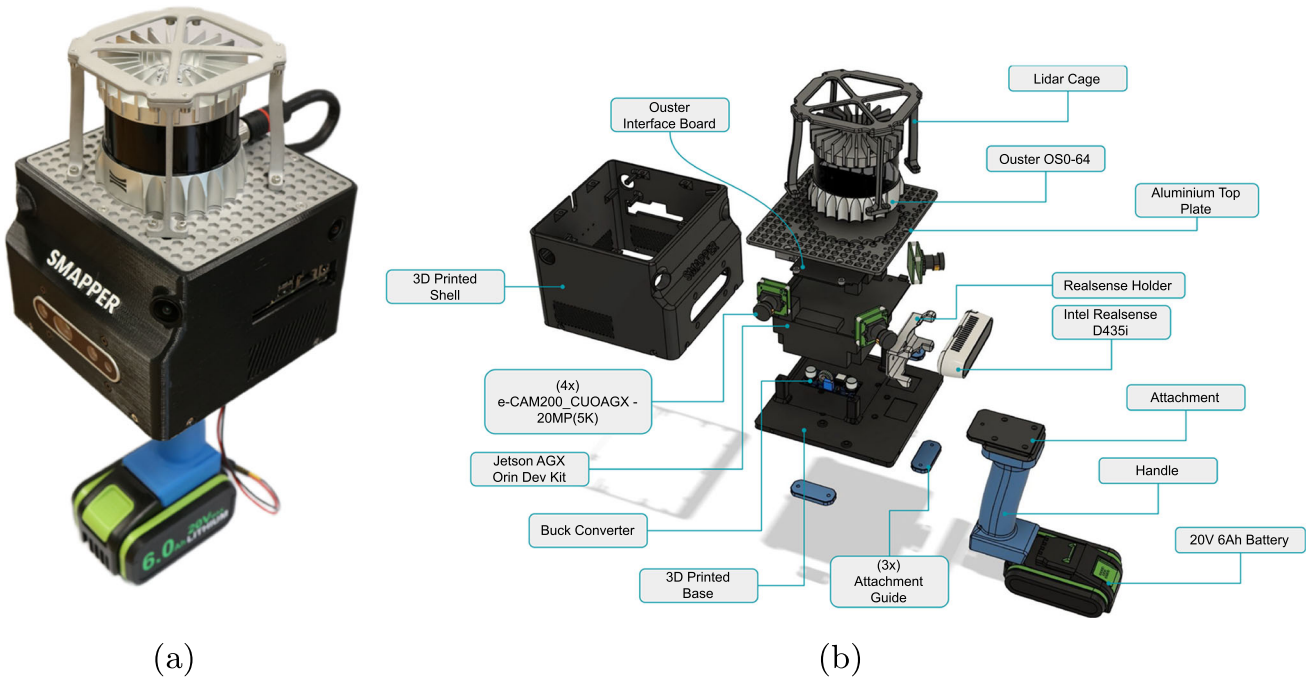

Fig. 1 Overview of the *SMapper* platform: (**a**) the fully assembled physical prototype, (**b**) the system overview highlighting the integrated sensors, components, and design elements tailored for diverse SLAM scenarios

SLAM and VSLAM domains [12]. Datasets such as TUM RGB-D [8] and OpenLORIS [13] provide accessible benchmarks through simple setups (*e.g.,* handheld vision sensors or mobile robots), while others utilize custom multimodal platforms. Such platforms tightly integrate complementary sensing modalities, including LiDAR, vision, inertial, and GNSS, to tackle complex challenges in navigation, large-scale mapping, and multimodal fusion benchmarking.

Accordingly, the Newer College Dataset [14] was collected using a hand-carried platform integrating a RealSense camera, a 64-beam Ouster OS-1 3D LiDAR with embedded IMU, and an onboard Intel NUC[1]. It comprises seven outdoor sequences of different durations, capturing a range of trajectories that include loops, spins, and other challenging motion patterns. While offering millimeter-accurate ground truth via a tripod-mounted survey-grade scanner, the setup faces challenges in terms of limited Field of View (FoV) and sensor synchronization. To address these, Zhang *et al.* [15] extended this dataset by incorporating a 128-beam Ouster OS-0 and a four-camera Alphasense kit, enhancing FoV and spatiotemporal resolution[2]. The resulting dataset remains confined to a few outdoor sequences with varying trajectories, motion aggressiveness, and scene complexity. Another recent contribution is the Oxford Spires dataset [16], collected using a custom-built multi-sensor perception unit in combination with a millimetre-accurate map obtained from a Terrestrial LiDAR Scanner (TLS). The dataset comprises 24 indoor and outdoor sequences covering a range of challenging scenarios and environmental conditions[3]. The perception unit integrates a 64-beam Hesai QT64 LiDAR, three global-shutter Alphasense Core fisheye cameras, and a synchronized IMU, all of which are precisely calibrated. Similarly, the Phasma device in the Hilti-Oxford Dataset [17] utilizes a 32-channel PandarXT-32 LiDAR, five infrared cameras, and an IMU. It includes a diverse set of sequences from indoor and outdoor construction sites, capturing a broad spectrum of challenging scenarios. A $Z+F$ Imager laser scanner is used to obtain prior maps of the environments as ground truth. However, this methodology faces high setup complexity and is less suited for dynamic, real-time environments.

PALoc [18] proposed a prior map-assisted framework for ground truth pose generation in LiDAR SLAM[4]. The device, supporting both handheld and robot-mounted configurations, captures dense 6-Degree of Freedom (DoF) trajectories across indoor and outdoor settings, but its reliance on monocular vision and LiDAR limits generalization to multimodal or vision-centric tasks. Inspired by PALoc, FusionPortableV2 [19] introduced a versatile multi-sensor platform for SLAM and autonomous driving data collection[5]. It integrates a 128-beam Ouster OS-1 LiDAR with IMU, two FLIR-BFS monochrome cameras, two DAVIS-346 event cameras, and a dual-antenna GNSS/Inertial Navigation System (INS) sensor. The dataset includes sequences captured in both indoor and outdoor environments, spanning handheld operation and deployments on legged robots, wheeled robots, and high-speed vehicles. While FusionPortableV2 enhances sensing richness, it faces high complexity in calibration and data alignment across modalities. In [20] the authors introduce DiTer, a diverse terrain dataset designed for ground mapping in construction robotics, covering a wide range of challenging terrain types such as sandy paths, vegetation, and sloped surfaces. The dataset was collected using a legged robot equipped with two RGB-D RealSense cameras, an Ouster OS-1 LiDAR with IMU, a GPS, and a FLIR Boson 640 thermal camera, providing rich multimodal sensory data. However, the dataset was not evaluated using either visual or LiDAR-based SLAM methods to verify its applicability in the domain. In another work, GEODE [21] provides a versatile robotics platform that integrates GNSS, motion capture, and multiple 3D laser scanners to support ground truth generation. While designed to address LiDAR degeneracies using diverse sensors, generalizing the platform introduced challenges in maintaining calibration and synchronization, causing increased sensitivity to synchronization drift. MapEval [22] focuses on standardizing evaluation for SLAM point cloud maps, emphasizing metrics for both global geometry and local consistency. It utilizes a simpler multi-sensor platform, comprising a 3D LiDAR and an SBG INS, primarily tailored for LiDAR-based SLAM scenarios. In addition to evaluating on the FusionPortableV2, Newer College, and GEODE datasets, the authors collected a 15-sequence in-house dataset. However, the platform requires careful adjustment of voxel size based on scene complexity and map density.

Table 1 summarizes the surveyed platforms and datasets that have significantly contributed to the field of SLAM datasets. The review of existing data collection platforms exposes a consistent trade-off inherent in their design. On one hand, platforms like FusionPortableV2 offer immense sensor richness but at the cost of high complexity in calibration and data management. On the other hand, simpler setups are more accessible but are often constrained by a limited number of sensor modalities or a narrow field of view. Furthermore, a common challenge across many of these systems is the complexity of the calibration and synchronization pipeline, which remains a significant barrier to practical use. Moreover, despite their value, only a limited number of platforms provide openly available hardware designs or software tools,

[1] https://ori-drs.github.io/newer-college-dataset/stereo-cam/

[2] https://ori-drs.github.io/newer-college-dataset/multi-cam/

[3] https://dynamic.robots.ox.ac.uk/datasets/oxford-spires/

[4] https://github.com/JokerJohn/PALoc

[5] https://fusionportable.github.io/dataset/fusionportable_v2/

Table 1 Various multimodal devices and platforms designed for collecting SLAM datasets. Terrestrial LiDAR Scanner (TLS) and Motion Capture System (MCS) denote common sources of ground truth data

Device/Dataset	Year	Ground Truth	Sensor Modality				Platform		Environment	Openness	
			Vision	*Depth*	*LiDAR*	*IMU*	*Handheld*	*Robot*	*Variant*	*Hardware*	*Tools*
TUM RGB-D [8]	2012	MCS	✓	✓	✗	✓	✓	✓	indoor	✗	✓
OpenLORIS [13]	2020	LiDAR + MCS	✓	✓	✓	✓	✗	✓	indoor	✗	✓
Newer College [14]	2020	LiDAR	✓	✓	✓	✓	✓	✗	outdoor	✗	✗
Zhang et al. [15]	2021	LiDAR	✓	✗	✓	✓	✓	✗	outdoor	✗	✗
Hilti-Oxford [17]	2022	Laser Scanner	✓	✓	✓	✓	✓	✗	in/outdoor	✗	✗
DiTer [20]	2024	LiDAR	✓	✓	✓	✓	✗	✓	outdoor	✗	✗
PALoc [18]	2024	MCS	✓	✗	✓	✓	✓	✓	in/outdoor	✗	✓
FusionPortable [19]	2024	Laser Scanner	✓	✓	✓	✓	✓	✓	in/outdoor	✗	✓
GEODE [21]	2024	LiDAR + MCS	✓	✓	✓	✓	✓	✓	in/outdoor	✗	✓
MapEval [22]	2025	Laser Scanner	✗	✗	✓	✓	✓	✓	in/outdoor	✗	✓
Oxford Spires [16]	2025	TLS	✓	✗	✓	✓	✓	✓	in/outdoor	✗	✗
SMapper (ours)	2025	LiDAR	✓	✓	✓	✓	✓	✓	in/outdoor	✓	✓

which restricts reproducibility and hinders broader adoption within the research community.

To bridge these gaps and achieve a balance between affordability, reproducibility, and sensor fusion, we introduce *SMapper*: a compact, tightly synchronized multimodal data collection platform tailored for SLAM benchmarking as well as broader robotics research. Unlike prior efforts limited by narrow sensor modalities or complex calibration pipelines, *SMapper* integrates a multi-camera setup with a wide overlapping FoV, enabling robust perception across diverse environments. The platform supports both handheld and robot-mounted use cases, designed for ease of calibration and extensibility, facilitating the collection of high-quality, reproducible datasets. Furthermore, we release the open-hardware design, open-source calibration and acquisition software, and a set of publicly available dataset instances to demonstrate the platform's practicality for SLAM benchmarking.

3 System Overview

As shown in Fig. 1, *SMapper* integrates various components and sensors within a modular structure that supports both *handheld* use (via a detachable handle mounted to the base) and *direct mounting* for ground robots. The sensors and companion computer are rigidly housed in a custom-designed, 3D-printed base, topped with an aluminum plate that serves as the mounting platform for the LiDAR and its protective cage. The complete system weighs $\sim$ 2.5kg (or 1.7kg without the handle and battery). It features a compact form factor of approximately 15cm $\times$ 15cm $\times$ 38.4cm (or 15cm $\times$ 15cm $\times$ 19.2cm without the handle and battery), enabling convenient single-handed operation. The *SMapper* device is equipped with an auxiliary onboard NVIDIA Jetson AGX Orin Developer Kit computer. This high-performance embedded computer enables efficient sensor data synchronization, real-time data recording and processing, and potential on-device inference. It is powered by an NVIDIA GPU with 2048 NVIDIA CUDA cores and a 12-core Arm Cortex-A78AE 64-bit CPU, making it well-suited for demanding robotics applications.

3.1 Sensors

Table 2 summarizes the specifications of the computing unit and sensors integrated into the *SMapper* device. According to the table, the device simultaneously captures data from various sources, supporting multimodal data acquisition. The platform includes a 64-beam Ouster OS0 3D LiDAR, offering a 100-meter range and an ultra-wide 360 $\times$ 90° coverage. Designed for short-range, high-precision perception, this sensor captures fine geometric details, making it well-suited for mobile robotics and widely adopted in LiDAR-based

Table 2 An overview of the hardware, including sensors and the embedded computer employed in the *SMapper* device

Hardware	Type	Rate	Characteristics
LiDAR	Ouster OS0	10/20 Hz	64 Channels, 100m Range FoV: 360° × 90° Resolution: 1024 × 64
Cameras	4× e-CAM200 CUOAGX	30 Hz	Rolling shutter, RGB FoV: 90° × 66° Resolution: 2K Synchronized
	Intel Realsense D435i	30 Hz	Global shutter, RGB-D FoV RGB: 69° × 42° FoV Depth: 87° × 58° Resolution: 2K Synchronized
IMU	LiDAR IMU	100 Hz	3-axis Gyroscope 3-axis Accelerometer
	Camera IMU	400 Hz	3-axis Gyroscope 3-axis Accelerometer
Onboard Computer	Jetson AGX Orin Developer Kit	1.3 GHz (Processor)	CPU: 12-core ARM GPU: NVIDIA 2048-core Memory: 64GB Vision/DL Accelerator

SLAM research. The device captures visual data from two sources: a forward-facing Intel RealSense D435i camera for recording RGB-D data, and four synchronized e-CAM200 CUOAGX electronic rolling-shutter cameras. The RealSense is mounted with a 0-degree pitch angle. The e-CAM200 cameras are particularly designed as a multi-vision solution for the Jetson computer, offering synchronization and consistent exposure for accurate multi-source perception. Integrating two types of visual sensors enables the platform to support a broad spectrum of robotic perception tasks, from depth-based analysis to multi-view geometry, and to simplify the benchmarking of diverse visual processing pipelines. While the FoV of the RealSense camera is $69^\circ \times 42^\circ$, the strategically placed e-CAM200 cameras extend the coverage to approximately $270^\circ \times 66^\circ$, offering a wide field suitable for situational awareness tasks. This configuration also produces an overlapping FoV of 30° among front and side e-CAM200 cameras.

It should be noted that the e-CAM200 CUOAGX cameras used in the device are fully interchangeable with other vision sensors, as long as they mechanically fit within the device's cage design. The primary reason for choosing these cameras is that they integrate seamlessly with the NVIDIA Jetson AGX Orin platform. While the rolling-shutter version of these cameras is supported in the default firmware, the same camera sensors can be replaced with their global-shutter variants at an additional cost. Although the *SMapper* device is primarily designed for handheld use or legged-robot mounting, the global-shutter camera version is essential for collecting data on a fast-moving platform. Furthermore, the device also incorporates a **RealSense D435i**, which provides a global-shutter RGB–D sensing option for applications that require distortion-free imaging.

Moreover, *SMapper* utilizes the built-in IMUs of the LiDAR and RealSense camera, providing three-axis gyroscope and accelerometer measurements with the angular velocity up to 400 Hz and linear acceleration up to 200 Hz for more robust pose estimation while recording data.

3.2 Synchronization Procedure

As an essential performance aspect of heterogeneous sensing, temporal synchronization ensures that measurements from different modalities are aligned within a shared time frame. This alignment is crucial for consistent data fusion, particularly in dynamic environments where even slight temporal offsets can result in significant errors in perception, mapping, and localization. The device supports three selectable timestamping modes:

- `TIME_FROM_PTP`: For the highest fidelity, the system supports Precision Time Protocol (PTP) as the foundation for temporal alignment across sensors. The NVIDIA Jetson Orin AGX is configured as the PTP grandmaster clock, establishing a high-precision time reference for the system. The Ouster LiDAR operates as a PTP slave synchronized via `linuxptp`, enabling both LiDAR point clouds and the integrated IMU to be timestamped directly in the PTP domain at the hardware level.
- `TIME_FROM_TSC`: For the multi-camera array, the CUOAGX camera driver implements PTP-aligned timestamping through a different mechanism. Each camera frame is initially stamped with the Jetson's hardware Time Stamp Counter (TSC) at the moment of acquisition. The driver then converts these TSC timestamps into the PTP time domain using NVIDIA's system interface, which maintains the correspondence between the TSC and PTP clocks. While this approach does not constitute native PTP hardware synchronization, it provides a consistent time reference aligned with the PTP grandmaster, suitable for multi-sensor fusion applications.
- `TIME_FROM_ROS`: The RealSense D435i depth camera and its integrated IMU represent a synchronization limitation of the current platform. Since no supported method was found to synchronize the RealSense sensor streams to an external PTP clock, these streams are timestamped using the Robot Operating System (ROS) system clock at message reception. This may introduce additional latency and jitter compared to PTP-synchronized sensors. However, owing to the driver's low-latency, event-driven architecture, this mode provides sufficiently accurate timestamps for most use cases with minimal configuration effort.

It should be added that a primary design decision in *SMapper* is to provide accurately timestamped raw sensor streams rather than pre-bundled synchronized ROS messages. This choice reflects the fact that modern SLAM frameworks implement their own synchronization strategies, which are specifically optimized for working with raw data. Pre-bundling at the driver level would reduce flexibility in applying custom synchronization policies and significantly increase storage requirements due to redundant data duplication. By aligning raw data streams to a high-precision standard clock, *SMapper* ensures temporal consistency while providing a compatible, storage-efficient data format, thereby maximizing its utility across diverse SLAM pipelines.

3.3 Calibration Procedure

Sensor calibration is essential to the practical usability and accuracy of *SMapper*, as precise spatio-temporal calibration forms the foundation for reliable data fusion and downstream SLAM tasks. To address this, we developed a comprehensive IMU-centric calibration pipeline, equipped with automation

tools to streamline the process, and complemented by multi-faceted validation to ensure the reliability of the results. As illustrated in Fig. 2, which depicts the spatial arrangement of the onboard sensors and their coordinate frames, the base module, cameras, LiDAR, and IMU are each associated with distinct reference frames. Defining these configurations is essential for accurate sensor fusion and consistent pose estimation in multimodal perception tasks. In this paper, we demonstrate both the manual `Kalibr`-based procedure (§3.3.1) and our automated calibration framework (§3.3.2), highlighting how the latter simplifies the process while maintaining accuracy and repeatability.

3.3.1 Manual Calibration

Accordingly, a robust, multi-step pipeline was developed based on the widely used `Kalibr` toolbox [23], which uses the high-frequency IMU as a standard "*bridge*" to link the different sensor modalities. The calibration pipeline consists of the following steps:

1. *IMU noise characterization*: A 20-hour static dataset was recorded using the Ouster and RealSense IMUs independently. The data were processed with the `allan_variance_ros` tool [24] to estimate gyroscope and accelerometer noise density (white noise) and bias instability (random walk). These parameters are the critical inputs for the `Kalibr` optimization process and subsequent state estimation algorithms.
2. *Camera intrinsic and extrinsic calibration*: This stage estimates each camera's internal parameters (intrinsics) and its rigid 3D pose relative to a reference IMU (extrinsics). A rigid 6×6 AprilTag grid (80×80 cm^2) [25] was used as the calibration target, with data collected by manually moving the device to capture the board from diverse viewpoints. The `Kalibr` toolbox [23] was employed to jointly optimize the camera intrinsics (focal length, principal point, distortion) and the camera-to-IMU transformations. For the four e-CAM200 cameras, extrinsics were computed relative to the Ouster IMU. In contrast, for the RealSense sensor, both its RGB camera and integrated IMU were calibrated against the Ouster IMU, yielding consistent transformations across modalities.
3. *Assembling the full transformation tree*: The final step integrates all calibration results into a unified transformation tree for the device. The camera-to-IMU trans-

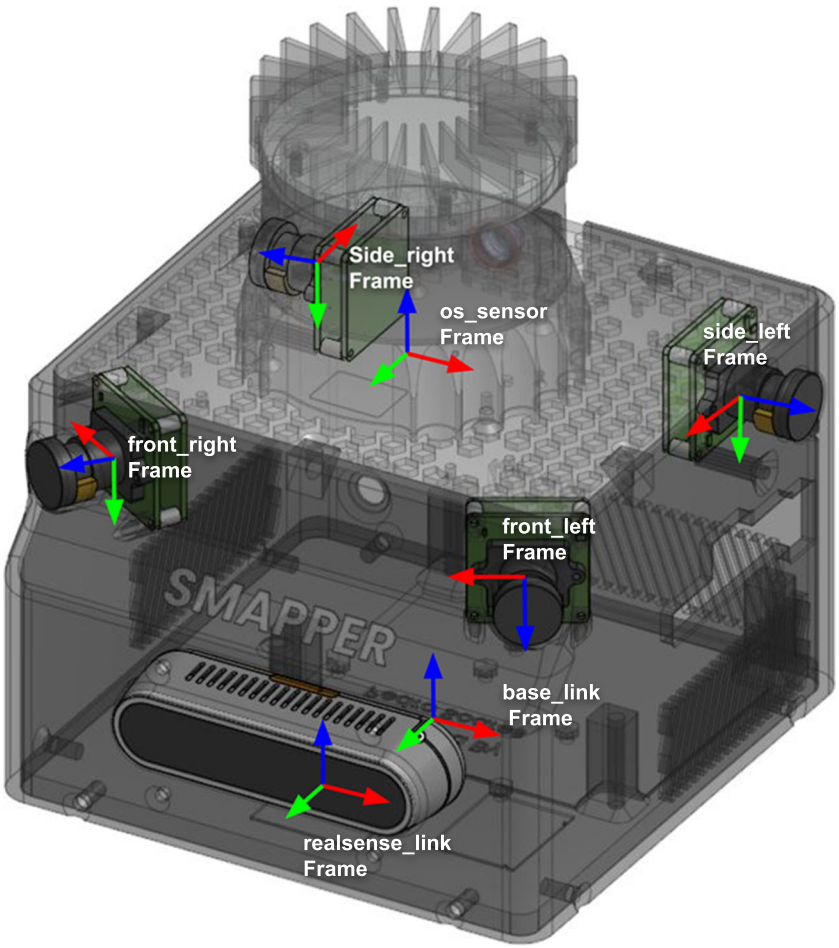

Fig. 2 Coordinate frames of the *SMapper* device, containing the spatial configuration of the cameras, LiDAR, and IMU sensors. The device contains the following coordinate systems: the base, RealSense D435i, e-CAM200 cameras, LiDAR, LiDAR IMU, and RealSense IMU

Table 3 Direct LiDAR–camera calibration results obtained from the `direct_visual_lidar_calibration` toolbox. ΔT and Δr denote the optimizer's final update magnitudes in meters and radians, respectively

Camera	*Cost*	*Translation* $[x, y, z]$ (m)	*Euler Angles* $[X, Y, Z]$ (deg)	ΔT (m)	Δr (rad)
Front Left	2.892	[0.027, 0.042, -0.020]	[89.20, 0.57, 120.75]	0.020	0.035
Front Right	2.896	[0.029, -0.045, -0.015]	[88.92, -0.17, 58.52]	0.014	0.035
Side Left	2.899	[-0.068, 0.069, -0.0225]	[89.25, 0.63, 179.48]	0.007	0.035
Side Right	2.850	[-0.047, -0.011, -0.089]	[90.66, -0.46, 0.97]	0.066	0.035

formations estimated by `Kalibr` are chained with manufacturer-provided extrinsics (*e.g.,* the known offset between the LiDAR and IMU frames), generating the precise 3D pose of every sensor relative to the `base_link` frame.

These calibrated sensor streams, including camera feeds, LiDAR point clouds, and inertial measurements, are published during data collection using the *SMapper* device. Additional technical details, documentation, and setup instructions for calibration procedures are publicly available at https://snt-arg.github.io/smapper_docs/.

3.3.2 Automated Calibration

The manual `Kalibr`-based calibration workflow is often complex, repetitive, and error-prone. To overcome these challenges, we developed the `smapper_toolbox`, a Python command-line utility that fully automates the process. The framework is publicly available in https://github.com/snt-arg/smapper_toolbox. Configured through a simple `YAML` file, the toolbox provides a Dockerized environment for executing each stage of the pipeline, including `ROS2-to-ROS1` bag conversion for compatibility with `Kalibr`, execution of intrinsics, and the generation of a ready-to-use `ROS2` launch file that publishes the device's static transforms. The output includes a complete Transformation Tree (TF) for the device, enabling the calibrated sensor poses to be readily integrated into downstream SLAM pipelines. This automation streamlines calibration into a robust, accessible, and repeatable process, representing a key contribution of *SMapper*.

In addition to the IMU-centric `Kalibr` pipeline, a dedicated LiDAR–camera calibration pipeline is achieved using the publicly available `direct_visual_lidar_calibration` toolbox [6] [26]. A quantitative evaluation of the generated extrinsics after seven optimization iterations is presented in Table 3. Accordingly, the method directly aligns LiDAR intensity/geometry with camera images at the pixel level, specifically designed to obtain high-precision extrinsics from natural scene structure. The solver converged with only minor corrective updates, with translation adjustments of $0.7 - 6.6$ cm and rotation updates of approximately 2°. These refinements are within the range commonly reported in state-of-the-art direct LiDAR–camera calibration literature.

3.3.3 Quantitative Validation

Three quantitative and qualitative checks were performed to validate the calibration results. First, the **reprojection error** reported by `Kalibr` was used to assess the internal consistency of the optimization. As shown in Table 4, all cameras achieved low mean reprojection errors, indicating a high-quality solution. Second, the calibrated extrinsics were compared against the nominal sensor placements from the `CAD` model. As shown in Table 5, the slight deviations between design specifications and estimated values confirm that the results are physically plausible. Finally, a visual validation was conducted using a custom point cloud colorization tool, which projects LiDAR points onto the image planes of the nearest cameras. The resulting colored point cloud (Fig. 3) shows strong geometric–visual alignment, with only minor residual offsets of a few centimeters, highlighting both the calibration's accuracy and opportunities for further refinement.

4 Benchmarking

To validate the platform's practicality for SLAM research, we collected representative datasets across diverse environments and conducted benchmarking experiments using state-of-the-art algorithms. The primary goal of these experiments is not only to demonstrate the platform's compatibility with established SLAM pipelines but also to evaluate its ability to generate reliable, high-fidelity datasets for assessing accuracy, robustness, and semantic understanding in real-world scenarios.

4.1 Baselines

The benchmarking was conducted using representative frameworks from both LiDAR- and vision-based SLAM approaches. For LiDAR SLAM, we employed *GLIM* [27], a state-of-the-art LiDAR–IMU odometry system known for its efficiency

[6] https://github.com/koide3/direct_visual_lidar_calibration

Table 4 Mean reprojection errors from the `Kalibr` extrinsic calibration, reported in *pixels*

Camera	*Reference IMU*	*Reprojection Error (Mean ± Std)*
Front Left	Ouster OS0	0.34 ± 0.46
Front Right	Ouster OS0	0.34 ± 0.34
Side Left	Ouster OS0	0.43 ± 0.52
Side Right	Ouster OS0	0.35 ± 0.38
RealSense	RealSense D435i	0.64 ± 0.60

and accuracy, along with *S-Graphs* [28, 29], which extends LiDAR-based SLAM by integrating semantic 3D scene graphs directly from point clouds. For visual SLAM, we utilized *ORB-SLAM3* [30], a widely recognized framework that supports various sensor configurations, and *vS-Graphs* [31], the vision-based version of *S-Graphs* that augments the reconstructed map with structured 3D scene graph representations. The generated map quality is quantitatively analyzed to understand how different systems perform across scenarios with varying sensor configurations and environmental challenges.

4.2 Data Collection

Data collection was conducted using the handheld configuration while traversing university campus buildings and sparsely populated areas at varying walking and turning speeds. The resulting dataset encompasses a diverse range of scenarios, from complex indoor environments with varied architectural layouts to spacious outdoor spaces. It should be noted that manual operation by a human operator introduced natural vibrations due to pedestrian motion. The collected sequences serve as representative samples to demonstrate the platform's capabilities, while the primary aim of this paper is to introduce the device itself rather than to establish a large-scale SLAM dataset. The characteristics of the collected dataset instances are summarized in Table 6, while representative examples are illustrated in Fig. 4.

The dataset is publicly available under the title *SMapper-light* for research and reproducibility purposes at https://huggingface.co/datasets/snt-arg/smapper-light. It contains six `rosbag` sequences, each with synchronized feeds from cameras, an IMU, and a LiDAR. To provide a reliable reference trajectory, we adopt a LiDAR-based SLAM approach executed in offline mode. While this approach does not constitute **absolute ground truth** through a dedicated external system, offline processing enables the accumulation of dense point clouds and achieves sub-centimeter accuracy (errors less than 3cm). Furthermore, the dense LiDAR reconstructions generated during this process are included in the dataset, providing users with transparent access to the underlying geometric information. This results in a reliable 6-DoF reference trajectory, along with dense 3D maps included with the dataset, sufficient for benchmarking both visual and multimodal SLAM pipelines. Moreover, the dense point clouds generated during the process are released as part of the dataset, providing researchers with high-fidelity 3D reconstructions of the environments, which can be employed for tasks beyond SLAM, such as scene graph generation or cross-modal learning.

4.3 Experimental Results

Benchmarking of the collected dataset is performed through qualitative and quantitative experiments. The qualitative evaluations (§4.3.1) involve visual inspections of the reconstructed map and trajectories, while the quantitative assessments assess (§4.3.2) the practicality of the dataset for visual SLAM. It should be noted that our objective is not to iden-

Table 5 Comparison of extrinsic parameters of the primary camera array: `CAD` model vs. `Kalibr` estimates with Euler angles and differences

Camera	*Source*	*Translation* $[x, y, z]$(m)	*Euler Angles* $[X, Y, Z](^\circ)$	*Position* Diff. (m)	*Angular* Diff. (°)
Front Left	`CAD`	[0.046, 0.057, 0.087]	[134.8, -45.4, -44.8]	0.018	1.98
	`Kalibr`	[0.061, 0.064, 0.085]	[133.6, -44.6, -46.0]		
Front Right	`CAD`	[0.046, -0.057, 0.087]	[45.4, -90.0, 0.0]	0.013	1.04
	`Kalibr`	[0.057, -0.063, 0.085]	[44.6, -89.9, 1.2]		
Side Left	`CAD`	[-0.057, 0.054, 0.087]	[180.0, 0.0, -90.0]	0.035	0.95
	`Kalibr`	[-0.060, 0.088, 0.080]	[179.2, -0.7, -89.7]		
Side Right	`CAD`	[-0.057, -0.054, 0.087]	[0.0, -90.0, 90.0]	0.025	1.02
	`Kalibr`	[-0.064, -0.077, 0.079]	[0.7, -89.5, 89.3]		

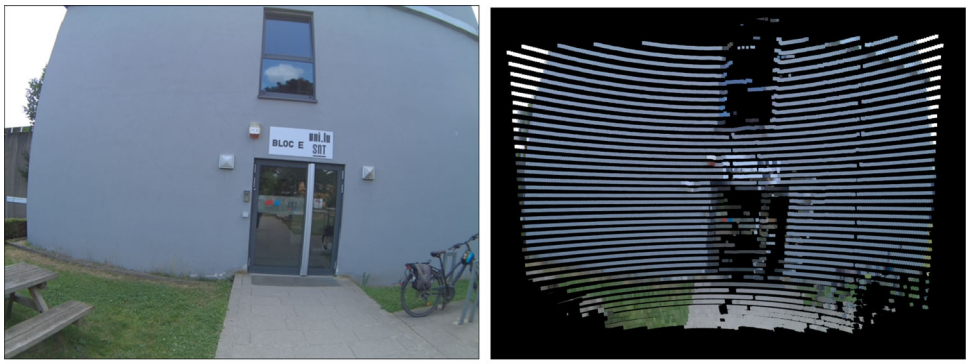

Fig. 3 Qualitative calibration validation using point cloud colorization with the `front-right` camera. (**a**) raw camera image; (**b**) LiDAR point cloud colored by the projected image. While the alignment is generally consistent, minor misalignments are visible at building edges, reflecting residual calibration errors

Table 6 The characteristics of the collected dataset, titled *SMapper-light*. All sequences are stored as `ROS` bag files in the `.mcap` format, containing synchronized data streams from all onboard sensors

Scenario	*Instance*	*Length*	*Duration*	*Size*	*Description*
Indoor	`IN_SMALL_01`	16.4m	01m 29s	5.7 GB	Single-room environment
	`IN_MULTI_01`	50.2m	06m 46s	13.5 GB	Multi-room linear trajectory
	`IN_MULTI_02`	84.3m	07m 07s	13.0 GB	Multi-room with loop closure
	`IN_LARGE_01`	204.3m	09m 30s	57.9 GB	Large-scale indoor with loop
Outdoor	`OUT_CAMPUS_01`	120.6m	04m 57s	36.4 GB	Urban campus linear path
	`OUT_CAMPUS_02`	141.2m	05m 15s	37.8 GB	Urban campus circular path
Total		617m	35m 04s	164.3 GB	

Fig. 4 Sample instances of *SMapper-light* dataset scenarios

tify which SLAM framework performs best, but rather to showcase the applicability of *SMapper-light* in the SLAM domain.

4.3.1 Qualitative Experiments

Figure 5 depicts the qualitative analysis of the various SLAM frameworks (including LiDAR-based and visual variants) used in the paper. Accordingly, the visual reconstructions of the environments highlight the strengths and limitations of the employed methodologies. In this regard, LiDAR-based approaches present denser maps owing to their highly reliable LiDAR trajectories. Among them, *S-Graphs* further improves the reconstructed maps through geometric reasoning to identify semantic structures, such as walls and rooms, and integrate them into the optimization process. In contrast, visual SLAM methodologies generate sparser reconstructions due to their reliance on visited visual features. However, these approaches can capture visual and appearance-driven information to augment the maps, as can be seen in vS-Graphs outputs, which extend this capability by incorporating semantic validation during map reconstruction. Overall, these observations confirm that the proposed dataset encompasses diverse scenarios, enabling various SLAM frameworks to showcase their respective mapping and optimization capabilities. This also validates the suitability

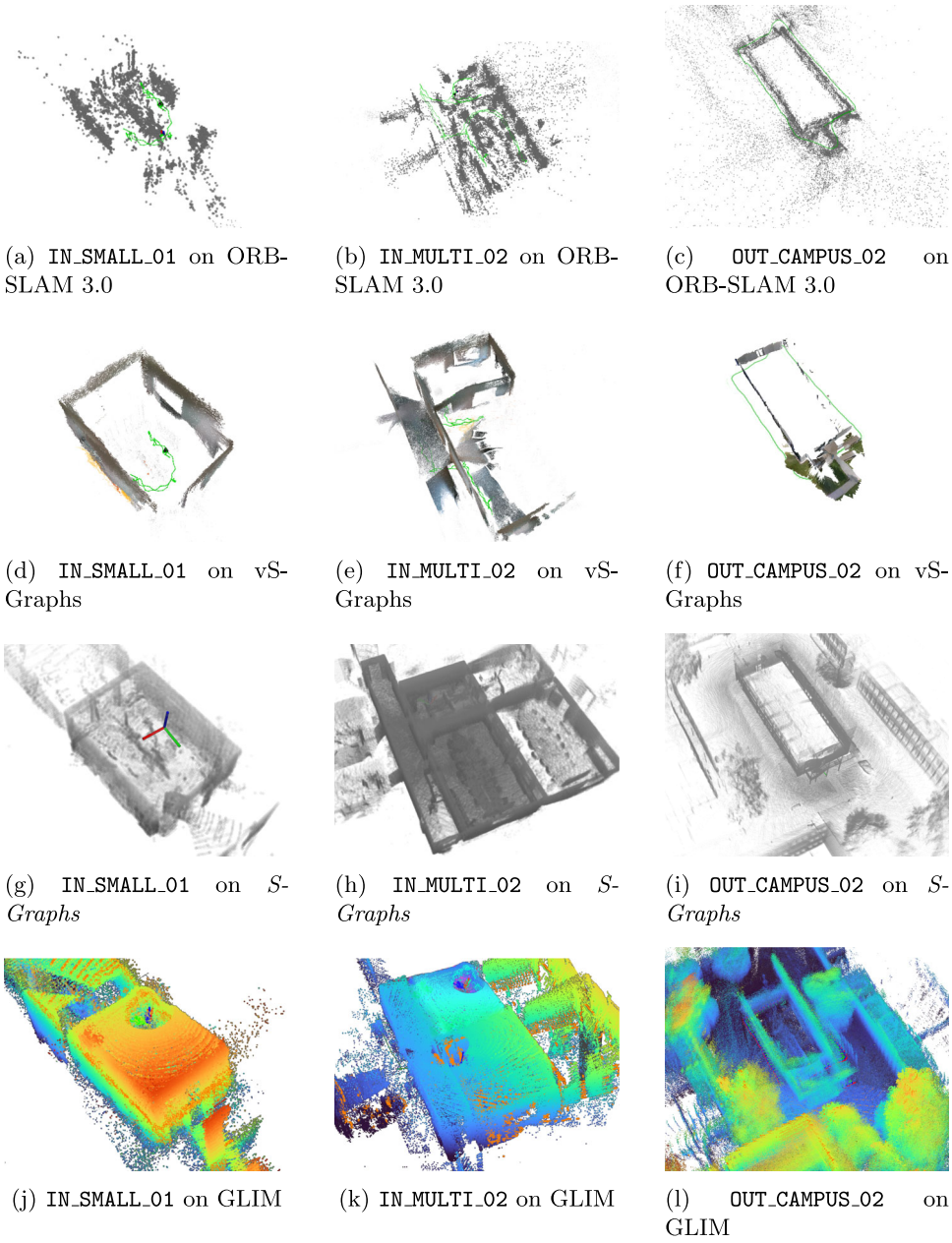

(a) IN_SMALL_01 on ORB-SLAM 3.0 (b) IN_MULTI_02 on ORB-SLAM 3.0 (c) OUT_CAMPUS_02 on ORB-SLAM 3.0

(d) IN_SMALL_01 on vS-Graphs (e) IN_MULTI_02 on vS-Graphs (f) OUT_CAMPUS_02 on vS-Graphs

(g) IN_SMALL_01 on *S-Graphs* (h) IN_MULTI_02 on *S-Graphs* (i) OUT_CAMPUS_02 on *S-Graphs*

(j) IN_SMALL_01 on GLIM (k) IN_MULTI_02 on GLIM (l) OUT_CAMPUS_02 on GLIM

Fig. 5 Qualitative results of SLAM benchmarking across selected sequences using various SLAM pipelines, including LiDAR-based (*S-Graphs* [28] and GLIM [27]) and visual SLAM (ORB-SLAM 3.0 [30] and vS-Graphs [31])

of the *SMapper* device for data collection and benchmarking purposes.

4.3.2 Quantitative Experiments

Table 7 presents the quantitative evaluation results obtained from the *SMapper-light* dataset. In this regard, the LiDAR-based SLAM trajectory generated by *S-Graphs* serves as the ground truth reference, against which the visual SLAM approaches are benchmarked. The analysis focuses on two primary metrics: the Root Mean Square Error (RMSE) and the Standard Deviation (STD) of the trajectory alignment, both expressed in meters.

According to the table, both *ORB-SLAM 3.0* and *vS-Graphs* demonstrate competitive accuracy across the indoor and outdoor sequences. *ORB-SLAM 3.0* generally performs better in shorter or less complex trajectories, benefiting from stable feature tracking and effective loop closure detection. In contrast, *vS-Graphs* relies heavily on the reliable recognition of environment-driven semantic entities, and fast rotations or missed detections can lead to mapping inconsistencies and reduced accuracy. Nevertheless, when semantic entities are correctly identified, particularly in multi-room and visually complex scenarios, integrating semantic validation within its optimization pipeline enables more coherent and structured reconstructions.

Overall, the relatively low RMSE and STD values across diverse environments confirm that the collected dataset provides well-calibrated, temporally aligned, and reliable multimodal measurements for visual SLAM benchmarking. This further supports the use of the proposed dataset as a practical resource for evaluating and comparing SLAM frameworks under realistic conditions.

4.4 Discussions

In general, data collection using *SMapper* is tailored to a balance between "portability" and "stability." While handheld use of the device enables flexible capture in confined spaces, robot-mounted data collection ensures smoother trajectories at the cost of mobility. The *SMapper-light* dataset (summarized in Table 6) comprises 615m of trajectories across indoor and outdoor environments. It serves as a **proof of concept** to demonstrate the versatility of *SMapper* and the practicality of its data acquisition and processing pipelines. Rather than aiming for large-scale coverage, the sequences were intentionally designed to capture a variety of structural layouts and environment-driven conditions that represent typical SLAM evaluation scenarios. Incorporating longer trajectories, dynamic environments, or specialized configurations remains open for other researchers to explore.

Additionally, an essential aspect of *SMapper* lies in its **open-hardware** nature, which promotes reproducibility and facilitates collaborative extensions. The released CAD models, calibration tools, and firmware configurations allow researchers to replicate or modify the system for specific sensing setups, bridging the gap between dataset usage and generation. In this regard, the device can be replicated for data collection, with or without ground truth (for testing purposes), lowering barriers to experimentation and accelerating dataset creation and benchmarking. While many existing SLAM datasets rely on expensive, proprietary, and difficult-to-reproduce sensor rigs, *SMapper* directly offers a **reconstructible**, **affordable**, and **transparent** platform. As the robotics community increasingly recognizes open hardware as a contribution [32–35], having *SMapper* can lead to a wide range of research opportunities, from studying cross-modal calibration to developing robust SLAM frameworks.

In terms of ground truth generation, the proposed LiDAR-based offline solution in *SMapper-light* primarily supports the evaluation of visual and visual–inertial SLAM systems and is not directly applicable to LiDAR-based SLAM methods. Generating accurate trajectories is often challenging because conventional approaches frequently rely on costly equipment, such as terrestrial laser scanners. To address this, several alternative strategies can be explored within the *SMapper* framework. For instance, augmenting the environment with fiducial markers placed at known positions enables pose estimation through multi-camera tracking, albeit at the cost of increased setup effort and potential visual artifacts in the dataset. Another direction is to integrate Building Information Models (BIMs), when available, to provide structural

Table 7 Evaluation results on the collected dataset using Root Mean Square Error (RMSE) error in *meters* and Standard Deviation (STD). Best results in each metric are boldfaced

Instance	RMSE		STD	
	ORB-SLAM 3.0	*vS-Graphs*	*ORB-SLAM 3.0*	*vS-Graphs*
IN_SMALL_01	**0.059**	0.072	**0.015**	0.024
IN_MULTI_01	0.347	**0.260**	0.198	**0.189**
IN_MULTI_02	0.123	**0.117**	**0.050**	0.056
IN_LARGE_01	**0.353**	0.381	0.215	**0.178**
OUT_CAMPUS_01	0.474	**0.434**	**0.206**	0.251
OUT_CAMPUS_02	**0.318**	0.534	**0.213**	0.390

priors for trajectory estimation. Although such solutions are beyond the scope of this paper, they can lay the foundation for extending the dataset to benchmark multi-sensor SLAM pipelines.

5 Conclusion

This paper presented *SMapper*, an open-hardware, multi-sensor platform designed to support reproducible research in SLAM and related fields. The device integrates synchronized LiDAR, multi-camera, and inertial sensing, supported by a robust calibration and synchronization pipeline that ensures accurate spatio-temporal alignment across modalities. Its fully open and replicable design allows researchers to extend its capabilities and deploy it across handheld or robot-mounted configurations. To validate the platform, we additionally introduced *SMapper-light*, a publicly available SLAM dataset containing representative indoor and outdoor sequences. The dataset includes tightly synchronized multimodal data, ground truth trajectories generated through offline LiDAR-based SLAM with sub-centimeter accuracy, and dense 3D reconstructions. Benchmarking experiments with state-of-the-art LiDAR and visual SLAM frameworks demonstrated the practicality and utility of the platform for evaluating diverse approaches.

Future work includes the expansion of *SMapper-light* into a comprehensive dataset covering both handheld and robot-mounted usage across a wide variety of indoor and outdoor environments. Another improvement involves the integration of external ground truth measurements, such as motion capture systems or terrestrial laser scans, to facilitate the creation of high-precision dataset sequences suitable for benchmarking multi-sensor SLAM frameworks.

Author Contributions Methodology, PM.BS., JL.SL., M.FC; writing—original draft preparation, PM.BS., A.T., M.FC.; writing—review and editing, A.T., M.FC., and JL.SL.; supervision, H.V. and JL.SL.; data collection and preparation, PM.BS, A.T. and A.BN.

Funding This research was funded, in whole or part, by the Luxembourg National Research Fund (FNR), DEUS Project, ref. C22/IS/17387634/DEUS. In addition, it was partially funded by the Institute of Advanced Studies (IAS) of the University of Luxembourg through an "Audacity" grant (project TRANSCEND - 2021).

Data Availability The dataset presented in this study is openly available at https://huggingface.co/datasets/snt-arg/smapper-light.

Code Availability The hardware design, software tools and documents are publicly available at https://snt-arg.github.io/smapper_docs/.

Declarations

Competing Interests The authors declare no competing interests.

References

1. Bavle, H., Sanchez-Lopez, J.L., Cimarelli, C., Tourani, A., Voos, H.: From slam to situational awareness: Challenges and survey. Sensors **23**, 4849 (2023)
2. Liu, Y. et al.: Simultaneous localization and mapping related datasets: A comprehensive survey. (2021) arXiv:2102.04036
3. Lluvia, I., Lazkano, E., Ansuategi, A.: Active mapping and robot exploration: A survey. Sensors **21**, 2445 (2021)
4. Zhang, Y., Shi, P., Li, J.: 3d lidar slam: A survey. Photogram. Rec. **39**, 457–517 (2024)
5. Macario Barros, A., Michel, M., Moline, Y., Corre, G., Carrel, F.: A comprehensive survey of visual slam algorithms. Robotics **11**, 24 (2022)
6. Geiger, A., Lenz, P., Stiller, C., Urtasun, R.: Vision meets robotics: The kitti dataset. The Int. J. Robot. Res. **32**, 1231–1237 (2013)
7. Burri, M., et al.: The euroc micro aerial vehicle datasets. The Int. J. Robot. Res. **35**, 1157–1163 (2016)
8. Sturm, J., Engelhard, N., Endres, F., Burgard, W. & Cremers, D.: A benchmark for the evaluation of rgb-d slam systems 573–580 (2012)
9. Terblanche, J., Claassens, S., Fourie, D.: Multimodal navigation-affordance matching for slam. IEEE Robot. Automat. Lett. **6**, 7728–7735 (2021)
10. Duan, S., Shi, Q., Wu, J.: Multimodal sensors and ml-based data fusion for advanced robots. Adv. Intell. Syst. **4**, 2200213 (2022)
11. Sier, H., et al.: A benchmark for multi-modal lidar slam with ground truth in gnss-denied environments. Remote. Sens. **15**, 3314 (2023)
12. Tourani, A., Bavle, H., Sanchez-Lopez, J.L., Voos, H.: Visual slam: What are the current trends and what to expect? Sensors **22**, 9297 (2022)
13. Shi, X. et al.: Are we ready for service robots? the openloris-scene datasets for lifelong slam. 3139–3145 (2020)
14. Ramezani, M. et al.: The newer college dataset: Handheld lidar, inertial and vision with ground truth. 4353–4360 (2020)
15. Zhang, L., Camurri, M., Wisth, D. & Fallon, M.: Multi-camera lidar inertial extension to the newer college dataset. (2021) arXiv:2112.08854
16. Tao, Y. et al.: The oxford spires dataset: Benchmarking large-scale lidar-visual localisation, reconstruction and radiance field methods. The Int. J. Robot. Res. 02783649251369905
17. Zhang, L., et al.: Hilti-oxford dataset: A millimeter-accurate benchmark for simultaneous localization and mapping. IEEE Robot. Automat. Lett. **8**, 408–415 (2022)
18. Hu, X., et al.: Paloc: Advancing slam benchmarking with prior-assisted 6-dof trajectory generation and uncertainty estimation. IEEE/ASME Trans. Mechatron. **29**, 4297–4308 (2024)

19. Wei, H. et al.: Fusionportablev2: A unified multi-sensor dataset for generalized slam across diverse platforms and scalable environments (2024). arXiv:2404.08563
20. Jeong, S., Kim, H., Cho, Y.: Diter: Diverse terrain and multimodal dataset for field robot navigation in outdoor environments. IEEE Sens. Lett. **8**, 1–4 (2024)
21. Chen, Z. et al.: Heterogeneous lidar dataset for benchmarking robust localization in diverse degenerate scenarios (2024). arXiv:2409.04961
22. Hu, X. et al.: Mapeval: Towards unified, robust and efficient slam map evaluation framework. IEEE Robot. Automat. Lett. (2025)
23. Furgale, P., Rehder, J. & Siegwart, R.: Unified temporal and spatial calibration for multi-sensor systems. 1280–1286 (2013)
24. Buchanan, R.: Allan variance ros. https://github.com/ori-drs/allan_variance_ros
25. Olson, E.: Apriltag: A robust and flexible visual fiducial system. 3400–3407 (2011)
26. Koide, K., Oishi, S., Yokozuka, M. & Banno, A.: General, single-shot, target-less, and automatic lidar-camera extrinsic calibration toolbox. (2023) arXiv:2302.05094
27. Koide, K., Yokozuka, M., Oishi, S., Banno, A.: Glim: 3d range-inertial localization and mapping with gpu-accelerated scan matching factors. Robot. Auton. Syst. **179**, 104750 (2024)
28. Bavle, H., Sanchez-Lopez, J.L., Shaheer, M., Civera, J., Voos, H.: Situational graphs for robot navigation in structured indoor environments. IEEE Robot. Automat. Lett. **7**, 9107–9114 (2022)
29. Bavle, H., Sanchez-Lopez, J.L., Shaheer, M., Civera, J., Voos, H.: S-graphs+: Real-time localization and mapping leveraging hierarchical representations. IEEE Robot. Automat. Lett. **8**, 4927–4934 (2023)
30. Campos, C., Elvira, R., Rodríguez, J.J.G., Montiel, J.M., Tardós, J.D.: Orb-slam3: An accurate open-source library for visual, visual-inertial, and multimap slam. IEEE Trans. Rob. **37**, 1874–1890 (2021)
31. Tourani, A. et al.: vs-graphs: Integrating visual slam and situational graphs through multi-level scene understanding. (2025) arXiv:2503.01783
32. Foehn, P. et al.: Agilicious: Open-source and open-hardware agile quadrotor for vision-based flight. Sci. Robot. **7**, eabl6259 (2022)
33. Tschopp, F., et al.: Versavis—an open, versatile, multi-camera visual-inertial sensor suite. Sensors **20**, 1439 (2020)
34. Sa, I., et al.: Build your own visual-inertial drone: A cost-effective and open-source autonomous drone. IEEE Robot. Automat. Magaz. **25**, 89–103 (2017)
35. Markovic, L., et al.: Towards a standardized aerial platform: Icuas'22 firefighting competition. J. Intell. Robot. Syst. **108**, 52 (2023)

Pedro Miguel Bastos Soares received the bachelor's and master's degrees in computer science from the University of Luxembourg, in 2023 and 2025, respectively. As part of his undergraduate studies, he spent a semester with the Université catholique de Louvain in Belgium through the Erasmus program. Alongside his academic training, he gained practical experience with the Automation and Robotics Research Group, Interdisciplinary Centre for Security, Reliability, and Trust (SnT), University of Luxembourg. In this role, he contributed to the development of ROS software packages, task coordination, and CAD modeling, and provided research assistance with the Aero Laboratory.

Ali Tourani received the master's degree in computer engineering from the University of Guilan, Iran, in 2019. He is a Doctoral Researcher in computer science with the Automation and Robotics Research Group, Interdisciplinary Centre for Security, Reliability, and Trust (SnT), University of Luxembourg. During his Ph.D. studies, he is exploring solutions to enhance robotic intelligence and situational awareness, utilizing vision sensors and advanced visual perception techniques. He has acquired experience through both practical and research-oriented computer vision projects and has published his work in several well-recognized scientific venues. His research interests include computer vision, visual SLAM, situational awareness, and robotics perception.

Miguel Fernandez-Cortizas is a postdoctoral researcher at the Interdisciplinary Centre for Security, Reliability and Trust (SnT), University of Luxembourg. He received his Ph.D. degree in Automation and Robotics from the Universidad Politécnica de Madrid (UPM), where he was a member of the Computer Vision and Aerial Robotics Group. His research interests include autonomous aerial robotics, multi-robot systems, cooperative perception, and robotic situational awareness, with a particular focus on cognitive architectures for collective decision-making. He has served as project lead and core developer of Aerostack2, a modular software framework for autonomous aerial robots. He has participated in several international UAV competitions, including IMAV, ICUAS, MBZIRC and A2RL, where his teams received multiple awards.

Asier Bikandi-Noya is a Ph.D. student in Computer Science Automation and Robotics Research Group, Interdisciplinary Centre for Security, Reliability, and Trust (SnT), University of Luxembourg. He received his double master's degree in Robotics and Control Systems from the Mondragon Unibertsitatea (Spain) and Technische Universität Wien (Austria) in 2024. His primary research interests are visual SLAM, situational awareness, and 3D scene understanding.

Holger Voos received the Dipl.-Ing. degree in electrical engineering from Saarland University and the Dr.-Ing. degree in automatic control from the Technical University of Kaiserslautern, Germany. From 2000 to 2004, he was a Systems Engineer with Bodenseewerk Gerätetechnik GmbH, Germany, and a Project Manager in aerospace and robotics research and development. From 2004 to 2010, he was a Professor and the Head of the Mobile Robotics Laboratory, University of Applied Sciences Ravensburg-Weingarten, Germany. Since 2010, he has been a Full Professor with the University of Luxembourg and the Head of the Automation and Robotics Research Group, Interdisciplinary Centre for Security, Reliability and Trust (SnT). From 2020 to 2024, he was the Founding Course Director of the New Interdisciplinary Space Master (ISM) Program, Faculty of Science, Technology and Medicine (FSTM). He is the author or co-author of more than 300 publications, comprising books, book chapters, journal, and conference papers. His research interests include situational awareness and motion planning and control for autonomous vehicles and robots, and distributed and networked control and automation.

Jose Luis Sanchez-Lopez received the Ph.D. degree in robotics from the Technical University of Madrid, in 2017, with research stays at Arizona State University and LAAS-CNRS. He has been with the University of Luxembourg, with visiting periods at H-BRS, INRIA Rennes, and the University of Zaragoza. He is a Permanent Research Scientist with the University of Luxembourg and the Co-Head of its Automation and Robotics Research Group. He also teaching the bachelor's- and master's-Level Courses with the University of Luxembourg, and regularly engages in national outreach. This work has yielded over 110 peer-reviewed publications, one patent, and several open-source software components. He has served as PI, co-PI, and work-package leader in national and European research projects, and in industry-driven technology-transfer projects. He currently supervises five Ph.D. students as primary advisor and six as co-supervisor, and has co-supervised and mentored several others. His research focuses on advancing mobile robots—especially ground platforms and multirotor aerial systems—toward deeper situational awareness, smarter decision-making and planning, higher task-level autonomy, and natural human–robot interaction for robust operation in real, complex, and predominantly human-made environments. He contributes to the Scientific Community as a Proposal Evaluator, an associate editor for several journals, a IPC member for major conferences, a reviewer for top-tier venues, and the Ph.D. thesis examiner.

Authors and Affiliations

Pedro Miguel Bastos Soares[1] · Ali Tourani[1,2] · Miguel Fernandez-Cortizas[1] · Asier Bikandi-Noya[1] · Holger Voos[1,3] · Jose Luis Sanchez-Lopez[1]

✉ Jose Luis Sanchez-Lopez
joseluis.sanchezlopez@uni.lu

Pedro Miguel Bastos Soares
pedro.bastos@ext.uni.lu

Ali Tourani
ali.tourani@uni.lu

Miguel Fernandez-Cortizas
miguel.fernandez@uni.lu

Asier Bikandi-Noya
asier.bikandi@uni.lu

Holger Voos
holger.voos@uni.lu

[1] Automation and Robotics Research Group (ARG), Interdisciplinary Centre for Security, Reliability, and Trust (SnT), University of Luxembourg, L-1359 Luxembourg, Luxembourg

[2] Institute for Advanced Studies (IAS), University of Luxembourg, L-4365 Esch-sur-Alzette, Luxembourg

[3] Faculty of Science, Technology and Medicine, University of Luxembourg, L-4365 Esch-sur-Alzette, Luxembourg